Influence of Chain Ordering on the Selectivity of Dipalmitoylphosphatidylcholine Bilayer Membranes for Permeant Size and Shape

Tian-Xiang Xiang and Bradley D. Anderson
Department of Pharmaceutics and Pharmaceutical Chemistry, University of Utah, Salt Lake City, Utah 84112 USA

ABSTRACT The effects of lipid chain packing and permeant size and shape on permeability across lipid bilayers have been investigated in gel and liquid crystalline dipalmitoylphosphatidylcholine (DPPC) bilayers by a combined NMR line-broadening/dynamic light scattering method using seven short-chain monocarboxylic acids (formic acid, acetic acid, propionic acid, butyric acid, valeric acid, isovaleric acid, and trimethylacetic acid) as permeants. The experimental permeability coefficients are compared with the predictions of a bulk solubility diffusion model in which the bilayer membrane is represented as a slab of bulk hexadecane. Deviations of the observed permeability coefficients (P_m) from the values predicted from solubility diffusion theory (P_o) lead to the determination of a correction factor, the permeability decrement f ($= P_m/P_o$), to account for the effects of chain ordering. The natural logarithm of f has been found to correlate linearly with the inverse of the bilayer free surface area with slopes of 25 ± 2, 36 ± 3, 45 ± 8, 32 ± 12, 33 ± 4, 49 ± 12, and 75 ± 6 Å^2 for formic acid, acetic acid, propionic acid, butyric acid, valeric acid, isovaleric acid, and trimethylacetic acid, respectively. The slope, which measures the sensitivity of the permeability coefficient of a given permeant to bilayer chain packing, exhibits an excellent linear correlation ($r = 0.94$) with the minimum cross-sectional area of the permeant and a poor correlation ($r = 0.59$) with molecular volume, suggesting that in the bilayer interior the permeants prefer to move with their long principal axis along the bilayer normal. Based on these studies, a permeability model combining the effects of bilayer chain packing and permeant size and shape on permeability across lipid membranes is developed.

INTRODUCTION

The passive transport rates of small molecules across biological membranes are often explained, at least qualitatively, by means of a bulk-phase solubility diffusion model (Fettiplace and Haydon, 1980; Finkelstein, 1976; Hanai and Haydon, 1966; Paula et al., 1996). This model, which may be traced to the formulation of Overton's rules nearly a century ago (Overton, 1899), describes the permeation process in terms of the partitioning of the permeant into the membrane, followed by its diffusion through the membrane, where the properties of the membrane are assumed to be adequately represented by a bulk lipid (e.g., hydrocarbon) solvent. It is well known, however, that permeabilities across biological membranes and model lipid bilayers depend strongly on both the degree of lipid chain packing in the membranes (Lande et al., 1995; Worman et al., 1986; Xiang and Anderson, 1995b, 1997) and the size of the permeating solute (Stein, 1986; Walter and Gutknecht, 1986; Xiang and Anderson, 1994c). The effects of lipid chain packing on permeability are most clearly demonstrated by the dramatic increase in transmembrane transport rates that occurs because of a gel-to-liquid crystalline phase transition (Carruthers and Melchior, 1983; Jansen and Blume, 1995; Papahadjopoulos et al., 1973; Xiang and Anderson, 1997). Membranes that are more "ordered" as a result of polar headgroup composition, or because of increased cholesterol concentrations or lower temperatures, or monolayers under high lateral pressures have greater resistances to permeation than predicted from a bulk solubility diffusion model, often by orders of magnitude (Bar-On and Degani, 1985; Brahm, 1983; Finkelstein, 1976; Magin and Niesman, 1984; Peters and Beck, 1983; Sada et al., 1990; Todd et al., 1989a,b). A steep size selectivity is exhibited by both biological membranes and lipid bilayers, as noted by several groups, including Lieb and Stein (1969, 1971, 1986), Walter and Gutknecht (1986), and ourselves (Anderson and Raykar, 1989; Xiang and Anderson, 1994b). These phenomena also cannot be accounted for by bulk solubility diffusion theory.

Although substantial progress has been made recently, the molecular mechanisms responsible for the chain-ordering effects on permeability and the role of permeant size have not been well understood historically. It has been common to interpret both the effects of chain ordering on permeability (Lande et al., 1995) and the steep dependence of permeation rates on permeant size (Stein and Nir, 1971; Stein, 1986) exclusively in terms of changes in solute diffusivity within membranes. Walter and Gutknecht (1986) argued, for example, that the effects of solute size on partitioning into a bilayer membrane are unimportant on the basis of the similarity in solubility of short-chain *n*-alkanes in lipid bilayers (Miller et al., 1977). On the contrary, large size effects on solute partitioning into interphases are evident from the high resolution attainable in chromatographic

Received for publication 17 December 1997 and in final form 10 August 1998.

Address reprint requests to Dr. Bradley D. Anderson, Department of Pharmaceutics and Pharmaceutical Chemistry, University of Utah, Salt Lake City, UT 84112. Tel.: 801-581-4688; Fax: 801-585-3614; E-mail: banderson@deans.pharm.utah.edu.

0006-3495/98/12/2658/14 $2.00

separations on the basis of subtle differences in size and shape (Wise et al., 1981). More recently, others have shown both theoretically (Marqusee and Dill, 1986) and experimentally (DeYoung and Dill, 1988, 1990; Xiang and Anderson, 1995b) that increasing chain ordering within lipid bilayers substantially reduces solute partitioning into bilayers. These effects are particularly evident in the more ordered regions of the bilayer, as confirmed in neutron diffraction experiments (White et al., 1981) and molecular dynamics simulations (Marrink and Berendsen, 1994, 1996; Xiang and Anderson, 1998). Further complicating the situation, statistical mechanical theory recently developed by the authors (Xiang and Anderson, 1994a) and molecular dynamics simulations conducted in these laboratories (data not shown) suggest that the size selectivity in partitioning is amplified with increases in bilayer chain ordering.

These recent results suggest that structure-transport relationships developed solely on the basis of lipophilicity or hydrogen bonding potential without consideration of molecular size effects and the influence of bilayer composition (i.e., chain ordering) on these size effects may be unreliable. Walter and Gutknecht (1984) noted, for example, that literature data for the incremental free energy changes accompanying the addition of a methylene group to various homologous series of permeants derived from transport studies across a variety of model bilayer and biological membranes were highly variable, ranging from nearly zero to −900 cal/mol. In addition to the inappropriate treatment of unstirred layer effects in some of these studies pointed out by Walter and Gutknecht, the differences in membrane composition and complexity in terms of lipid chain packing (e.g., gel and liquid-crystalline phases) may also have contributed to the variability in the effects of permeant chain length on permeability.

A more systematic characterization of solute permeability with respect to the states of lipid packing in lipid bilayers is essential to a thorough understanding of molecular mechanisms for solute transport across biological membranes. The difficulties in investigating the effects of permeant size on permeability arise from the fact that changes in permeant size are usually accompanied by changes in lipophilicity, with the latter effects often overshadowing the effects of permeant size alone.

In this study we will investigate the effects of permeant size on membrane permeability in a way markedly different from previous studies. Namely, we will examine by means of an NMR line-broadening method the size and shape selectivity of dipalmitoylphosphatidylcholine (DPPC) bilayers for the transport of a series of seven monocarboxylic acids differing in chain length and degree of chain branching (Fig. 1) as a function of lipid bilayer packing, characterized by the bilayer free surface area. The use of a homologous series of monocarboxylic acids minimizes the effects of hydrogen bond potential on the analysis of solute shape and size effects. Our aim, in part, is to examine the hypothesis that increasing lipid chain order will be accompanied by increased membrane selectivity to permeant size and shape. To accomplish this we will apply a chain ordering correction factor to the bulk solubility-diffusion model predicted permeability coefficients to account for the discrepancies between the observed values and those calculated neglecting chain-ordering effects (Xiang and Anderson, 1997). We will then develop an empirical relationship between the permeability decrement due to chain ordering and the bilayer packing properties described by the membrane free surface area. The slope of the linear relationship between the natural logarithm of the chain-ordering correction factor (i.e., the permeability decrement) and the inverse

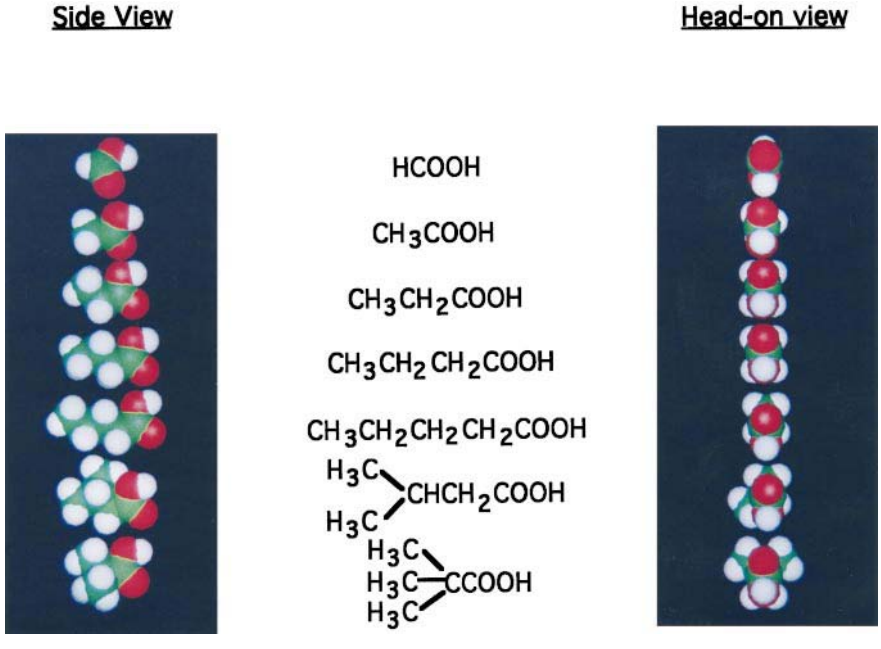

FIGURE 1 The side and head-on views of space-filling models of seven monocarboxylic acids used in this study as permeants. The area of the head-on view gives the minimum cross-sectional area of the molecule.

of free surface area will be shown to depend linearly on permeant size when expressed in terms of permeant cross-sectional area.

EXPERIMENTAL

Materials

DPPC was purchased from Avanti Polar Lipids (Pelham, AL). Formic acid (99%) and [^{14}C]formic acid (>98%) were purchased from Sigma Chemical Co. (St. Louis, MO). [^{3}H]Acetic acid, [^{14}C]propionic acid, and [^{14}C]butyric acid were obtained from American Radiolabeled Chemical (St. Louis, MO). Acetic acid (99.8%), propionic acid (99+%), butyric acid (99+%), valeric acid (99+%), isovaleric acid (99%), trimethylacetic acid (99%), deuterium oxide (99%), and hexadecane (99%) were purchased from Aldrich Chemical Co. (Milwaukee, WI). All other reagents were obtained commercially and were of analytical reagent grade. Polycarbonate membranes and membrane holders were obtained from Nuclepore (Pleasanton, CA).

Large unilamellar vesicle liposome preparation

A detailed description of the experimental procedure has been published elsewhere (Xiang and Anderson, 1995a). In brief, large unilamellar vesicles (LUVs) were prepared by a modified combined technique of Bangham et al. (1965) and Olson et al. (1979). The DPPC lipids were accurately weighed, dissolved in chloroform, evaporated to a dry thin film under nitrogen gas, and left under vacuum for 2 h at ~50°C. A deuterated aqueous solution containing 5–30 mM permeant was then added to a final lipid concentration of 10 mg/ml. The lipids were then hydrated by repeated vortexing and shaking above the main transition temperature (41°C). The multilamellar vesicles formed were then forced through a 0.1–0.2-μm polycarbonate membrane filter 18 times to form LUVs before the NMR transport experiments.

Permeability coefficient determinations

The permeability coefficients for the seven monocarboxylic acids across DPPC bilayers were determined at various temperatures by the ^{1}H-NMR line-broadening method developed by Alger and Prestegard (1979) and further validated in a recent study by the authors (Xiang and Anderson, 1995a). The experiments were performed on a Bruker-200 NMR spectrometer (Bruker Instruments, Billerica, MA) operated in the Fourier transform mode at 200 MHz. Samples were equilibrated for 20 min at a given temperature controlled by a standard variable-temperature accessory (BVT1000; Bruker). Each spectrum was the average of 32–1000 acquisitions separated by 2–5-s pulse delays. The spectra were Fourier transformed and phased with an Aspect 3000 computer. The resonance frequencies of selected protons in the permeants located inside and outside the vesicles, ω_i and ω_o, were separated by adding an impermeable shift reagent, $Pr(NO_3)_3$ (final concentration, 0.5–3 mM), to the sample before the spectral acquisitions. The binding capacity of the chemical shift reagent (Pr^{3+}) and its effects on solute permeability have been studied previously (Xiang and Anderson, 1995a). The DPPC main transition temperature was found to remain constant (41 ± 0.5°C) upon the addition of 5 mM Pr^{3+}, and the permeability coefficient for acetic acid in DMPC/CHOL was shown to be independent of [Pr^{3+}] up to 40 mM. The concentration of free Pr^{3+} available for binding to the outer vesicle surface is lower than the total Pr^{3+} concentration because of complex formation between carboxylic acids and Pr^{3+}. For example, at [Pr^{3+}] = 5 mM and an acetic acid concentration of 0.05 M (pD 6.32), only ~25% of the total Pr^{3+} would exist in the uncomplexed form.

The proton peak(s) for the methylene group adjacent to the carboxylic acid group in acetic acid, propionic acid, butyric acid, and valeric acid exhibit the greatest chemical shift in the presence of paramagnetic ions and thus were used for the permeability determinations. However, proton coupling in propionic acid, butyric acid, valeric acid, and isovaleric acid splits the proton resonances into two to four peaks, precluding an accurate determination of the line broadening due to solute transport. This was minimized by irradiating these protons through a separate decoupling channel. The collapsed singlet peak had a linewidth of 1.0–2.2 Hz in LUVs in the absence of chemical shift reagent. For isovaleric acid and trimethylacetic acid, the proton peak(s) for the methyl groups are the strongest and most symmetrical and thus were used for the permeability determinations.

The lifetime of the permeant inside the vesicle, τ_i, was obtained using the following linewidth expression in the slow exchange limit, $|\omega_i - \omega_o|T_{2,i} \gg 1$ (Piette and Anderson, 1959):

$$\pi\Delta\nu = 1/T_{2,i} + 1/\tau_i \tag{1}$$

where $\Delta\nu$ is the full linewidth at one-half the maximum peak height, and $T_{2,i}$ is the spin-spin relaxation time, which includes heterogeneous line broadening in the absence of exchange. The linewidth in the absence of exchange ($1/T_{2,i}$ = 2.6–5.0 Hz) was obtained at a low temperature and/or high pD, where the permeation rate is negligible.

Previous studies in these laboratories have shown that the permeabilities of ionized carboxylic acid permeants are negligible in the pD range of interest (Xiang and Anderson, 1995a). Thus the permeability coefficient for the neutral species, P_m, can be expressed as

$$P_m = \frac{V}{\tau_i A_t}\frac{([D^+] + K_a)}{[D^+]} \tag{2}$$

where V is the entrapped volume, A_t is the vesicle surface area, and K_a is the dissociation constant in D_2O. The V/A_t ratio was determined from the vesicle hydrodynamic diameter (d), as obtained from dynamic light scattering (DLS) measurements according to the formula $V/A_t = d/6$. DLS experiments were conducted with a goniometer/autocorrelator (model BI-2030AT; Brookhaven, Holtsville, NY) and an Ar^+ ion laser (M95; Cooper Laser Sonics, Palo Alto, CA) operated at 514.5-nm wavelength. One drop of LUV suspension was placed in a 13 × 75 mm cleaned glass test tube and brought to a volume of 2 ml with the same filtered buffer solution. The sample was placed in a temperature-controlled cuvette holder with a toluene index-matching bath. Autocorrelation functions were determined for a period of 100 s with a 10–80-μs duration at 90° and analyzed by the method of cumulants.

Partition coefficient determinations

Hexadecane/water partition coefficients for the series of monocarboxylic acids were measured using the shake flask method at a pH 2 units below the pK_a of the corresponding acid to ensure that >99% was in its unionized form. The organic solvent was first washed three times with an equal amount of de-ionized water. The organic solvent (2–3 ml) and 1 ml of an aqueous solution containing 3×10^{-2} to 1×10^{-4} M of "cold" permeant or 1–20 μCi of radiolabeled permeant were placed in a test tube and mixed with magnetic stirring in an incubator at a preset temperature (25–50°C) for 24 h. The sample was then centrifuged to remove any emulsified water from the organic phase. Aliquots of both phases were carefully taken for high-performance liquid chromatography (HPLC) analyses of "cold" compounds (acetic acid, propionic acid, butyric acid, valeric acid, isovaleric acid, and trimethylacetic acid) or for liquid scintillation counting (LS1801; Beckman Instrument Co., Fullerton, CA) of radiolabeled compounds (formic acid, acetic acid, propionic acid, and butyric acid). Duplicate measurements were performed with two different permeant concentrations to evaluate the effects of permeant self-association in hexadecane on the measured partition coefficients. To minimize the potential effects of more lipophilic impurities in the radiolabeled compounds (not a problem if HPLC is used for concentration analyses), the organic phase was replaced with fresh solvent, and the above experimental procedure was repeated until the radioactivity in the organic phase reached a

plateau value. The partition coefficient was calculated as the ratio between the molar concentrations in the hydrocarbon solvent and water.

The partition coefficients obtained using both "hot" and "cold" compounds and two different solute concentrations were generally within the experimental error, suggesting that self-association was not a significant factor in the partition coefficient determinations.

An HPLC system consisting of a syringe-loaded sample injector (Rheodyne model 7125; Rainin Instrument Co., Woburn, MA), a solvent delivery system (110B; Beckman Instrument Co., San Ramon, CA) operated at a flow rate of 1.0–1.2 ml/min, a dual-wavelength absorbance detector (model 441, Water Associates, Milford, MA) operated at 214 nm, an integrator (model 3392A; Hewlett-Packard Co., Avondale, PA), and a reversed-phase column packed with 5-μm C18 300 Å (Jupiter, 4.6 mm i.d. × 25 cm; Phenomenex Co., Torrance, CA) was used at ambient temperature for the analyses of the "cold" monocarboxylic acids taken during the partition experiments. Mobile phases containing 2.5%–40% acetonitrile, depending on the analyte lipophilicity, and 0.01 M phosphate buffer (pH 3.0) were employed.

pK_a determinations in D_2O

The ionization constants for the series of monocarboxylic acids in deuterated water were measured by a pD titration. An accurately weighed amount of each acid was dissolved in 2.0 ml D_2O to yield a final concentration of 0.03 M. pK_a determinations were carried out at 24°C under nitrogen by slow addition of 0.03 M NaOD while monitoring the apparent pH with a standard pH meter (PHM82; Radiometer, Copenhagen, Denmark) calibrated with standard buffer solutions. The pD values were obtained by adding 0.40 units to the corresponding pH readings (Glasoe and Long, 1960). Plots of the pD values versus the titrant volumes added were fitted numerically, including a correction for changes of the ionic strength using Davies' equation (Perrin and Dempsey, 1974). The dissociation constants obtained are presented in Table 1.

RESULTS AND DISCUSSION

Transport experiments were conducted in large unilamellar vesicles composed of DPPC. The chain packing properties within these DPPC bilayers, as characterized by the bilayer free surface area (see Eq. 8), were varied by changes in temperature, which also brought about changes in bilayer phase structure (gel and liquid crystalline phases). Seven monocarboxylic acids differing in chain length and the degree of chain branching as shown in Fig. 1 were used as permeants. This permeant series offered several advantages for the purposes of this study. One was the technical advantage of being able to determine the permeability coefficients for this series of relatively lipophilic permeants by the NMR line-broadening method, in contrast to other, slower transport methods that rely on separations of intravesicular permeants from the external solution (e.g., size exclusion chromatography, ultrafiltration, or dialysis). Moreover, the size and shape of permeants within this series could be varied in a more systematic manner. Furthermore, the structural changes involved only variations in the number of methylene groups, which have relatively small and well-documented effects on solute lipophilicity in comparison to most substituents. This rendered less problematic the selection of an appropriate bulk reference solvent to correct for the effects of changes in permeant lipophilicity on permeability, as the incremental free energy for the transfer of a single methylene group from water to various bulk organic solvents is essentially independent of the nature of the solvent (−849 cal/mol in heptane compared with −712 cal/mol in octanol; Davis et al., 1972, 1974).

Permeability coefficients: expectations from bulk solubility-diffusion theory

As noted earlier, bulk solubility-diffusion theory assumes that solute partitioning from water into and diffusion through a lipid bilayer or biomembrane resembles that within a homogeneous slab of bulk solvent such as olive oil, octanol, or hydrocarbon. The permeability coefficient predicted from this model (P_o) can be expressed as

$$P_o = \frac{K_{hc/w} D_o}{\delta} \tag{3}$$

TABLE 1 The total molecular volume (V_s), the cross-sectional area (a_s) along the long axis, the ionization constants (pK_a) in deuterated water, the apparent activation energies for permeation (E_a), and various thermodynamic properties for transfer from water to hexadecane for the monocarboxylic acids studied*

				E_a (kcal/mol)			Thermodynamic transfer parameters (water → hexadecane) (kcal/mol)		
Permeant	V_s (Å^3)#	a_s (Å^2)§	pK_a (D_2O)	Gel-phase DPPC	Liquid crystalline DPPC	Bulk-phase model	$\Delta G^\circ_{hc/w}$ (30°C)	$T\Delta S^\circ_{hc/w}$ (30°C)	$\Delta H^\circ_{hc/w}$
Formic acid	38.5	10.9	4.24 ± 0.04	21 ± 6	23 ± 2	10.3 ± 0.9	5.5 ± 0.2	−2.3 ± 0.5	3.2 ± 0.3
Acetic acid	61.2	13.0	5.11 ± 0.03	44 ± 7	39 ± 1	11.3 ± 0.8	4.8 ± 0.1	−0.65 ± 0.3	4.1 ± 0.2
Propionic acid	78.2	15.9	5.34 ± 0.02	60 ± 2	—	11.6 ± 1.0	3.6 ± 0.1	0.83 ± 0.4	4.4 ± 0.3
Butyric acid	95.2	16.1	5.30 ± 0.03	51 ± 9	—	11.9 ± 1.6	2.7 ± 0.0	2.0 ± 1.1	4.7 ± 1.1
Valeric acid	112.2	15.8	5.32 ± 0.02	49 ± 5	—	12.7 ± 0.9	2.0 ± 0.1	3.5 ± 0.4	5.4 ± 0.3
Isovaleric acid	112.2	20.8	5.30 ± 0.02	61 ± 8	—	12.6 ± 1.1	2.1 ± 0.2	3.3 ± 0.7	5.3 ± 0.5
Trimethylacetic acid	112.2	26.5	5.50 ± 0.02	74 ± 4	—	11.0 ± 1.1	1.7 ± 0.1	2.0 ± 0.5	3.7 ± 0.4

*Expressed as mean ± standard deviation.

#Calculated from an atomic increment method (Edward, 1970).

§Estimated from the space-filling model in the molecular graphic program, InsightII (Biosym).

where $K_{hc/w}$ and D_o are the organic solvent (i.e., hexadecane)/water partition coefficient and the diffusion coefficient in the organic solvent, respectively, and δ is the effective thickness of the homogeneous layer of organic solvent.

To use bulk solubility-diffusion theory to predict permeability coefficients as temperature is varied, the temperature dependence for permeant partitioning into (and diffusion through) an organic solvent that most closely mimics the physicochemical properties of the barrier domain in the bilayer membrane under investigation must be known. A large body of evidence has shown that the barrier domain in lipid bilayers behaves like a hydrocarbon solvent with respect to intermolecular electrostatic interactions (Stein, 1986; Xiang and Anderson, 1994c). Moreover, certain dynamic properties in the bilayer interior, including chain reorientation rates and microviscosity resemble those in bulk hexadecane (Bell, 1981; Brown et al., 1986; Venable et al., 1993). Thus hexadecane, which resembles the lipid chains in DPPC in terms of chain length and degree of saturation, was used as a model solvent in this study. Fig. 2 shows the Arrhenius plots of the hexadecane/water partition coefficients for the series of monocarboxylic acids used in this study. The molar free energies, enthalpies (obtained from the slopes of linear fits of the data in Fig. 2), and entropies of transfer from water to hexadecane are presented in Table 1. The transfer enthalpies ($\Delta H°$) are in the range of 3.2–5.4 kcal/mol and generally increase with the chain length, suggesting that permeant dehydration contributes only a small fraction of the large activation energies observed for permeability of the monocarboxylic acids across DPPC bilayers (vide infra). Increases in $\Delta H°$ with chain length were also found for the transfer of short-chain alkanols (C_1-C_5) from water to hydrocarbons (Nemethy et al., 1963). These values are approximations, as they are assumed to be constant over the entire temperature range explored (25–50°C). Large transfer heat capacities are typically observed (DeYoung and Dill, 1990), however, which may change the slopes of Arrhenius plots from which the molar enthalpies of transfer were obtained. The partition coefficient for valeric acid is slightly larger than that for isovaleric acid, which is consistent with the view that chain branching decreases the molecular surface area and thereby reduces the partition coefficient due to the reduced hydrophobic interaction in water (Grant and Higuchi, 1990). However, the partition coefficient for trimethylacetic acid is about twice as large as that for valeric acid, whereas $\Delta H°_{hc/w}$ is smaller for trimethylacetic acid. These results may be attributed to the fact that the three methyl groups in trimethylacetic acid may interfere with solvation of the carboxylic acid group by water, effectively making it less hydrophilic. Steric hindrance of solvation of the ion produced on ionization of highly hindered aliphatic acids also decreases acid strength (Hine, 1975), as demonstrated by a 0.2-unit higher pK_a value for trimethylacetic acid than that for valeric acid.

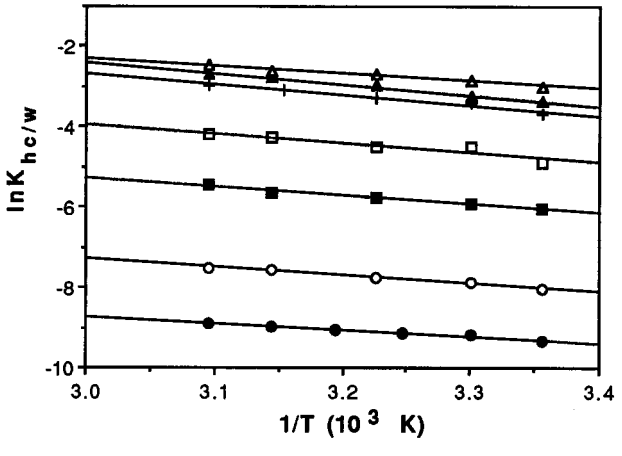

FIGURE 2 Arrhenius plots of the hexadecane/water partition coefficients for formic acid (●), acetic acid (○), propionic acid (■), butyric acid (□), valeric acid (▲), isovaleric acid (+), and trimethylacetic acid (△).

The diffusion coefficients of monocarboxylic acids in bulk solvents are determined primarily by their molecular sizes (Albery et al., 1967), whereas the polar carboxylic acid residue is expected to play a minor role, at least in nonpolar hydrocarbons (Chan, 1983). As a result, the diffusion coefficients for the monocarboxylic acids used in this study were estimated from a relation developed from the experimental diffusivity data for a series of alkane homologs in hexadecane at 25°C (Hayduk and Ioakimidis, 1976) and the assumption that the diffusion coefficient varies inversely with solvent viscosity:

$$D(\mathrm{cm^2/s}) = \frac{1.386 \times 10^{-3}}{\eta V_s^{0.8315}} \tag{4}$$

where η is the viscosity (cp) of hexadecane and V_s is the solute volume ($Å^3$). The molecular volumes for the series of diffusants were calculated from an atomic additivity method (Edward, 1970). The size dependence in Eq. 4 ($n = 0.83$) is stronger than that predicted by the Stokes-Einstein relation ($n = 0.33$), though less than that typically observed for solute diffusion in polymers ($n = 1.1$–3.8) (Lieb and Stein, 1969).

Because of the small changes of bilayer density with temperature, the thickness of the acyl chain region in the bilayer, δ, is related to the bilayer reduced surface density σ (vide infra) by $\delta = l_o\sigma$, where l_o (= 38.4 Å) is the end-to-end length of a fully extended DPPC molecule.

The permeability coefficients (P_o) from bulk solubility-diffusion theory are calculated at different temperatures by combining the sets of partition coefficients, diffusion coefficients, and bilayer thickness data described above. These results are presented in Fig. 3 for later comparison with the experimental permeability coefficients. Bulk solubility diffusion theory predicts a weak dependence of permeability on temperature, as indicated by the relatively small activation energies E_a derived from the slopes of the ln P_o versus $1/T$ data in Fig. 3, which are listed in Table 1 (10.3–12.7 kcal/mol).

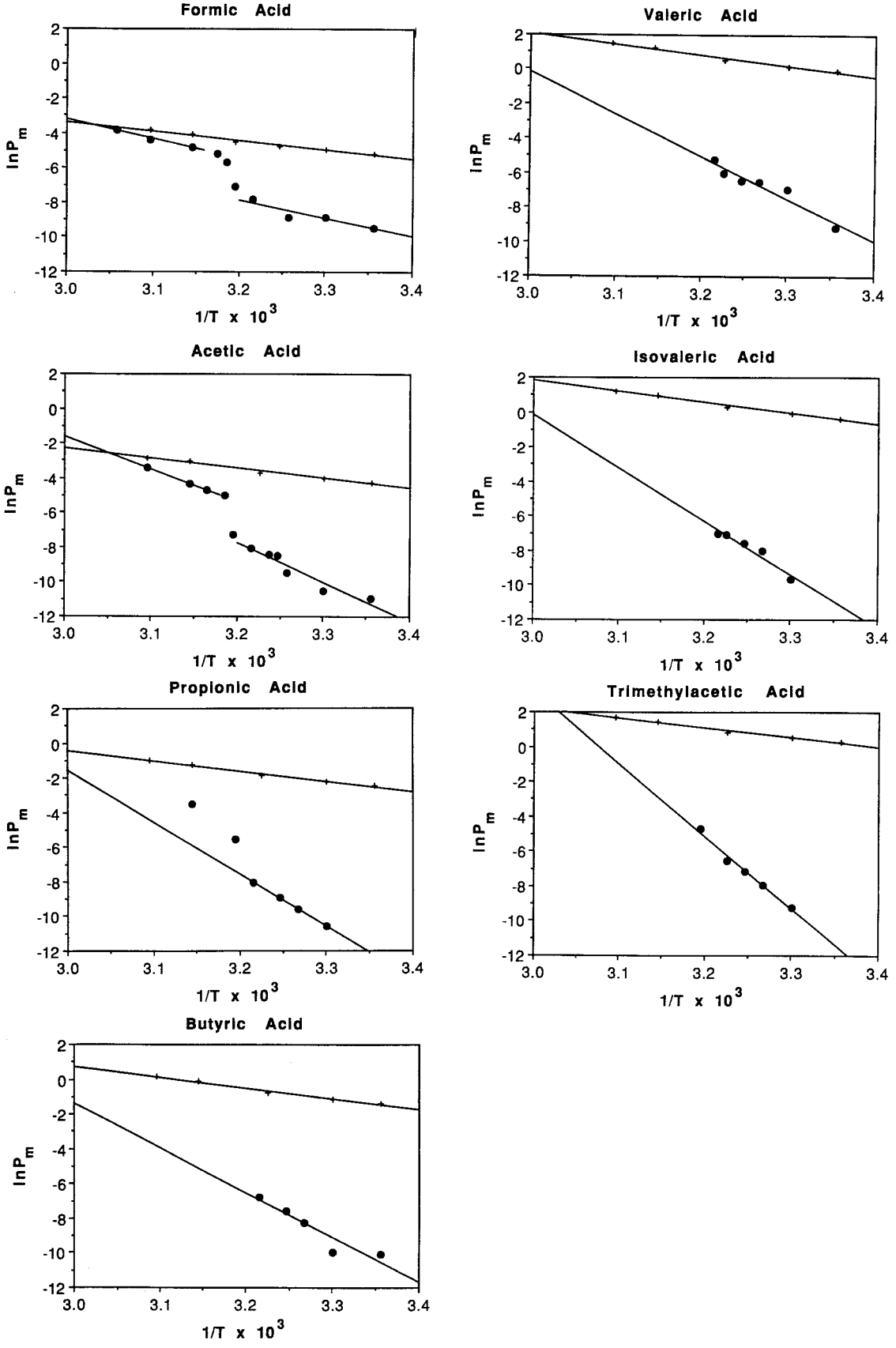

FIGURE 3 Arrhenius plots of the permeability coefficients for formic acid, acetic acid, propionic acid, butyric acid, valeric acid, isovaleric acid, and trimethylacetic acid across DPPC LUVs. ●, Experimental permeability coefficients (P_m); +, permeability coefficients predicted from bulk solubility-diffusion theory (P_o).

Membrane permeability coefficients: deviations from bulk solubility-diffusion theory

Fig. 4 shows the proton magnetic resonance peak(s) for the methylene group adjacent to the carboxylic group in butyric acid in DPPC LUVs in the absence and presence of chemical shift reagent (Pr^{3+}) and with and without coupling to the neighboring methylene group. In the absence of Pr^{3+}, decoupling of the methylene group by irradiating at a radio frequency corresponding to the central position of the adjacent methylene group leads to a narrow singlet peak (~1.5 Hz) for the methylene group (Fig. 4 *B*). Addition of Pr^{3+} shifts the proton peaks of the extravesicular permeant downfield (~140 Hz), whereas that of the permeant entrapped in the internal aqueous space is broadened (Fig. 4, *C* and *D*). The degree of line broadening, which is attributed to the exchange of permeant across the LUVs, was found to depend on pD and temperature. The permeability coefficient can be calculated according to Eqs. 1 and 2 from the observed linewidth and solution pD.

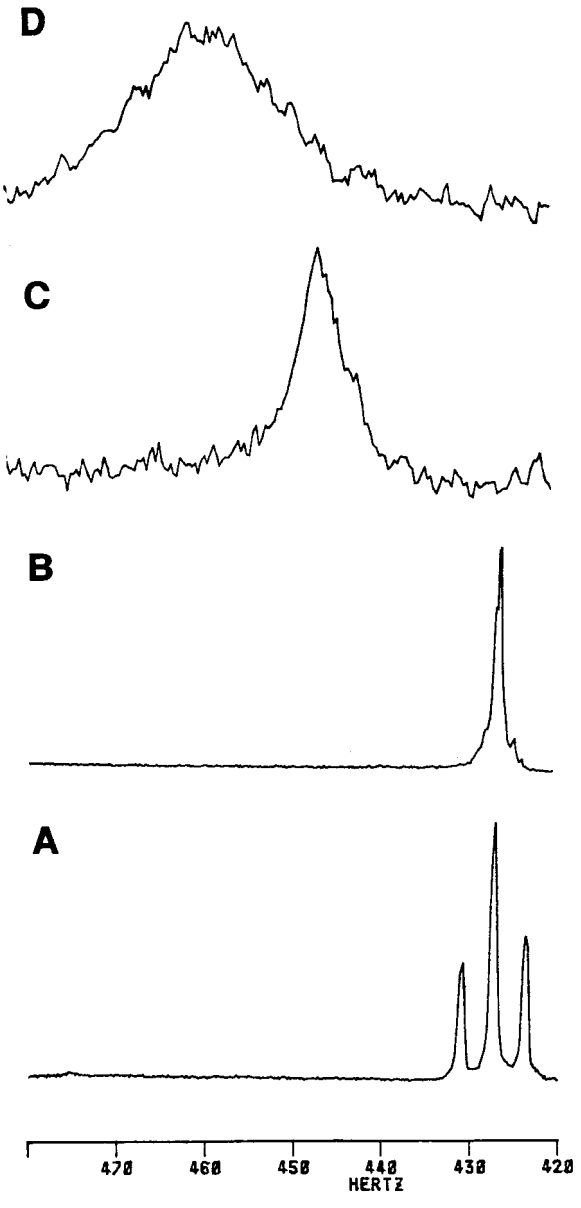

FIGURE 4 Proton magnetic resonances for the methylene group adjacent to the carboxylic group in butyric acid in DPPC LUVs at pD 6.09. (*A* and *B*) In the absence of chemical shift reagent and at 21°C. (*C*) In the presence of 2 mM Pr^{3+} at 32°C. (*D*) In the presence of 2 mM Pr^{3+} at 38°C. The decoupling power was off for the spectrum in *A* and on for the spectra in *B–D*. The sweep width was 2.8 kHz and the pulse width was 4.0 μs. The decouple width was 10 Hz.

Temperature dependence

Arrhenius plots of the permeability coefficients (P_m) for the series of monocarboxylic acids across DPPC bilayers are shown in Fig. 3, along with the solubility diffusion theory-predicted permeability coefficients (P_o) described earlier. Because of the abrupt increases in P_m at the main phase transition, linear least-squares fits of the permeability data were performed in the single-phase (gel or liquid crystalline) regions. Intravesicular proton peaks could not be detected for butyric acid, valeric acid, isovaleric acid, and trimethylacetic acid above the main phase transition in DPPC bilayers because of their higher permeation rates and the precipitation of their Pr^{3+} salts at pD $>$ 7.5. The apparent activation energies (E_a) obtained are listed in Table 1.

As is evident in Fig. 3, the experimental permeability coefficients deviate substantially from the predictions of the bulk solubility-diffusion model, with the extent of the deviation being highest at lower temperatures (i.e., in densely packed DDPC gel-state bilayers), where differences of more than four orders of magnitude are seen. At higher temperatures, well above the gel-to-liquid crystalline phase transition temperature, the experimental values remain below the solubility diffusion theory-predicted permeability coefficients, but because their temperature sensitivities are higher, it appears that they would converge with the solubility diffusion model predictions at a sufficiently high temperature.

The large activation energies obtained are also in contrast to $E_a \approx 10–13$ kcal/mol predicted from the bulk solubility diffusion model (Table 1). Previous studies in liquid crystalline bilayers have also reported higher values of E_a than bulk solubility-diffusion theory predicts for the transport of *n*-alkylamines ($\approx$ 20 kcal/mol in egg lecithin bilayers; Bar-On and Degani, 1985), glucose (26 kcal/mol in DMPC bilayers; Bresseleers et al., 1984), and polyhydroxy alcohols (14–25 kcal/mol in DMPC/cholesterol; de Gier et al., 1971). These results can be rationalized, as discussed later, by the effects of lipid chain ordering on permeability in both the gel and liquid crystalline phases. By analogy, higher activation energies (10–20 kcal/mol) are observed for the diffusion of small solutes in more densely packed polymers (e.g., polyisobutylene and natural rubber) than those in a simple fluid (Meares, 1965). The variability in activation energies in Table 1 is pronounced, ranging from 21 to 74 kcal/mol, with large increases in E_a evident from formic acid to acetic acid and from valeric acid to trimethylacetic acid. Qualitatively, there appears to be a correlation be-

tween the cross-sectional area of the permeant and energy of activation observed in gel-phase bilayer transport.

Methylene group contributions

The methylene group contribution to solute permeability across lipid bilayers and other biological membranes and to solute partitioning from water into various organic solvents has been studied extensively (Davis et al., 1972, 1974; Walter and Gutknecht, 1984). The incremental free energy change for the transfer of a single methylene group from water to various bulk organic solvents of relatively low polarity is not very sensitive to the choice of the homologous series of solutes employed or the nature of the solvent (e.g., −849 cal/mol in heptane compared with −712 cal/mol in octanol; Davis et al., 1972, 1974). This can be rationalized by the relative constancy of the London interactions between a methylene group and the solvent molecules and suggests that the choice of model bulk solvent for predicting the methylene group contribution to lipid bilayer permeability coefficients according to bulk solubility-diffusion theory is not very critical. A linear regression analysis of the natural logarithms of the hexadecane/water partition coefficients at 30°C (Fig. 2) versus chain length (not shown) yielded a value of −919 ± 41 cal/mol for the methylene group contribution to the free energy of transfer, in good agreement with the value of −898 ± 159 cal/mol reported by Walter and Gutknecht at 25°C, and representing an increase of 4.6-fold in the partition coefficient with each methylene group added. Although there is a slight decrease in the bulk diffusion coefficient with each successive methylene group added within an homologous series as described by Eq. 4, by far the greatest contribution to the predicted permeability according to Eq. 3 is from the partitioning term. For the monocarboxylic acid homologs, bulk solubility-diffusion theory predicts roughly uniform increases of approximately three- to fourfold in permeability coefficient per methylene group added to the permeant.

The apparent methylene group contribution to the free energy of transfer of a solute from water to the rate-determining barrier region of a lipid bilayer, $\delta\Delta G$, can be defined as

$$\delta\Delta G = RT\ln(P_{m,1}/P_{m,2}) \quad (5)$$

where $P_{m,1}$ and $P_{m,2}$ are the permeability coefficients for two permeants that differ by one methylene group. In contrast to the relatively narrow range of values observed for the methylene group contribution to solute partitioning in bulk solvent systems, however, the methylene group contribution derived from transport experiments in lipid bilayers and other biological membranes varies over a much wider range. A compilation of methylene group contributions by Walter and Gutknecht (1984) included values ranging from −118 ± 156 cal/mol in the jejunum (Sallee and Dietschy, 1973), −591 ± 133 cal/mol in red cell membranes (Klocke et al., 1972), and −679 ± 274 cal/mol in toad bladder membranes (Rosen et al., 1964) to −764 ± 54 cal/mol in model egg lecithin bilayers (Walter and Gutknecht, 1984). Although some of the variability may have arisen from inappropriate treatment of unstirred layer effects and the effects of metabolism, there have been no systematic studies to date that have explored the possibility that lipid chain ordering in the membranes may also contribute to large variability and to a reduced effective membrane hydrophobicity when probed by the methylene group contribution.

Fig. 5 displays the natural logarithms of the permeability coefficients of the monocarboxylic acids as a function of the number of carbon atoms, n, across DPPC bilayers in both the gel phase (30°C) and liquid crystalline phase (45°C). Also shown for comparison are the bulk solubility diffusion model-predicted values as a function of n at 30°C. The dependence of P_m on chain length changes markedly with the bilayer phase structure. In liquid crystalline DPPC bilayers at 45°C, an approximately monotonic increase in permeability coefficient with permeant chain length is evident, but with an apparent $\delta\Delta G$ (363 ± 82 cal/mol) substantially lower than expected from bulk solubility-diffusion theory and lower than that reported for egg lecithin bilayers at 25°C (764 ± 54 cal/mol; Walter and Gutknecht, 1984), which are more disordered at 25°C than DPPC bilayers at 45°C. A more complex pattern emerges in gel-phase DPPC bilayers at 30°C, where the permeability coefficient decreases with increasing chain length for short-chain monocarboxylic acids from formic acid to propionic acid, followed by a reversal in this trend at higher chain lengths. These results suggest that the methylene group contribution reflects both the lipophilicity of the permeant and the chain ordering within the membrane. In the densely packed gel phase, unfavorable steric interactions upon the addition of a

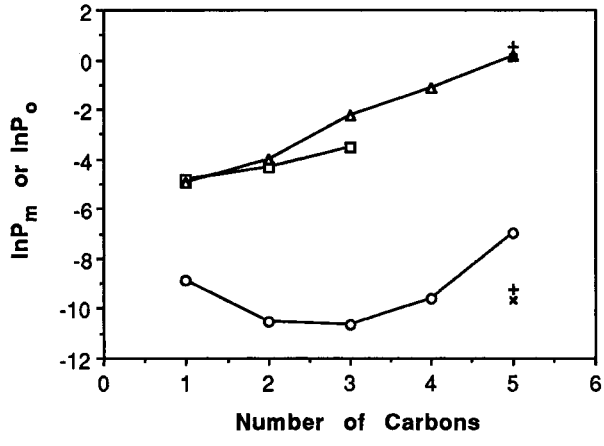

FIGURE 5 Dependence of the observed permeability coefficients (P_m) and those predicted from bulk solubility-diffusion theory (P_o) on the number of carbon segments in the permeants. ○, DPPC bilayers at 30°C (gel phase); □, DPPC bilayers at 45°C (liquid-crystalline phase); △, predicted P_o values at 30°C. The × and + symbols are for isovaleric acid and trimethylacetic acid, which have the same number of carbon segments as valeric acid.

methylene group to small permeants may dominate over the accompanying increase in lipophilicity.

Also shown in Fig. 5 are the permeability coefficients for isovaleric acid and trimethylacetic acid, as predicted by bulk solubility-diffusion theory and in DPPC gel-phase bilayers. The 10-fold and 14-fold lower permeability coefficients for trimethylacetic acid and isovaleric acid relative to valeric acid in the gel phase contrasts sharply with the predicted behavior from bulk solubility-diffusion theory, in which solute partitioning from water into hexadecane solvent is favored for trimethylacetic acid and only slightly disfavored for isovaleric acid. These results highlight in another way the inadequacy of bulk solubility-diffusion models in accounting for permeabilities in lipid bilayers.

The permeability decrement due to chain ordering depends on free surface area and permeant cross-sectional area

A large body of evidence from this and other laboratories (DeYoung and Dill, 1988, 1990; Xiang and Anderson, 1995b, 1997) indicates that the failure of homogeneous solubility diffusion theory to predict permeabilities in lipid bilayer membranes stems from the neglect of the effects of chain ordering in lipid membranes as characterized by order parameters and other related properties. We have previously shown that the permeability coefficient predicted from bulk solubility-diffusion theory must be adjusted downward by a factor f to correct for chain-ordering effects (Xiang and Anderson, 1997). Thus the permeability decrement due to chain ordering is defined as the ratio between the experimental and bulk phase model-predicted permeability coefficients:

$$f = \frac{P_m}{P_o} \tag{6}$$

We have recently proposed that the effects of bilayer packing on transbilayer permeabilities as quantified by f can be rationalized in terms of a dependence of permeability on the two-dimensional packing structure, as characterized by the free surface area per lipid molecule, a_f, as depicted below:

$$f = f_o \exp(-\lambda a_s/a_f) \tag{7}$$

where a_s is a characteristic cross-sectional area of solute and f_o and λ are constants independent of permeant size and bilayer packing structure. Similar to the definition of free volume (Bondi, 1954), the mean free surface area per lipid molecule is related to the area occupied by one phospholipid molecule, A, by

$$a_f = A - A_o = A_o(1/\sigma - 1) \tag{8}$$

where A_o (= 40.8 Å^2) is the area of a phospholipid molecule in the crystal (Tardieu et al., 1973) and σ (= A_o/A) is the reduced surface density. The surface density data, as reported in our previous work (Xiang and Anderson, 1997), were obtained from acyl chain order parameters (DeYoung and Dill, 1988; Morrow et al., 1992) based on the existence of one-to-one correspondence between these two bilayer properties, regardless of the chemical structure of the lipid (Boden et al., 1991; Nagle, 1993).

The model described by Eq. 7 predicts an inverse linear correlation between ln f and the free surface area. This prediction was verified in a study of the permeability of acetic acid in distearoylphosphatidylcholine, dipalmitoylphosphatidylcholine, dimyristoylphosphatidylcholine, and dilauroylphosphatidylcholine bilayers and their mixtures with cholesterol, at various temperatures both above and below the gel-to-liquid crystalline phase transition temperatures (Xiang and Anderson, 1997). The present study, employing permeants varying in molecular size, allows us to confirm the inverse dependence of ln f on a_f and to test another novel feature of this model, the dependence of the permeability decrement on the cross-sectional area rather than the molecular volume of the permeant.

Values of ln f calculated from the experimental (P_m) and bulk solubility-diffusion model predicted (P_o) permeability data for the series of monocarboxylic acids (cf. Fig. 3) are presented in Fig. 6 as a function of the membrane free surface area, a_f. The free surface area was varied by changes of temperature, which also induced changes in bilayer phase structure. Values of f vary from nearly 1 for the smallest permeant (formic acid) in liquid crystalline bilayers to $<1 \times 10^{-4}$ for the permeant with the greatest cross-sectional area, trimethylacetic acid, in a highly ordered gel-state bilayer. As noted in Fig. 6, approximately linear relationships are observed between ln f and the mean free surface area for all monocarboxylic acids studied. Least-squares fits of the permeability decrement data according to Eq. 7 are also shown in Fig. 6. The slopes and correlation coefficients obtained are listed in Table 2. The slope, which measures the sensitivity of the permeability coefficient of a given permeant to membrane chain ordering, increases significantly from formic acid to acetic acid, then remains approximately constant from acetic acid to valeric acid, and again increases significantly for isovaleric acid and trimethylacetic acid, two permeants that have the same number of carbons and molecular volume as valeric acid.

Fig. 1 displays space-filling models of the monocarboxylic acids used in this study, constructed with a molecular graphics program, Insight II (Biosym Technologies, San Diego, CA). Views from two different perspectives are shown. The cross-sectional areas along the long axes (i.e., the minimum cross-sectional areas) as represented by the "head-on view" in Fig. 1 are presented in Table 1. Values of the slopes obtained from the ln $f - A_o/a_f$ profiles in Fig. 6 are plotted versus the minimum cross-sectional areas of the monocarboxylic acid permeants in Fig. 7. A linear least-squares fit of the data yielded a slope of 0.072 Å^{-2}, with a 95% confidence range (S-plane) of 0.032–0.11 Å^{-2}, providing a value of λ = 2.7. Thus the slope is significantly different from zero. The excellent correlation of r = 0.94 is substantially higher than the correlation of r = 0.59 ob-

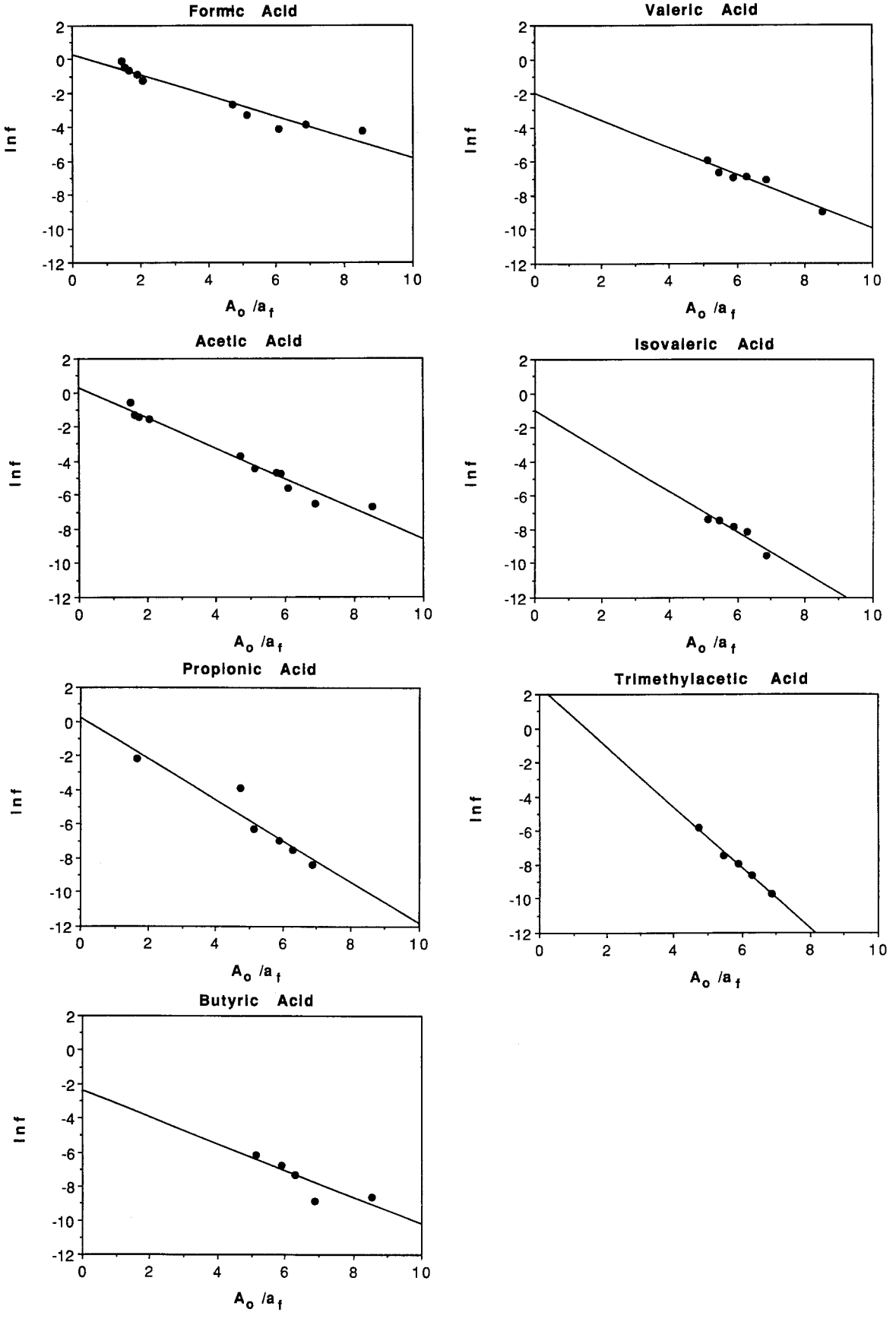

FIGURE 6 Natural logarithms of the permeability decrement, f, for formic acid, acetic acid, propionic acid, butyric acid, valeric acid, isovaleric acid, and trimethylacetic acid across DPPC bilayers versus the inverse of the reduced free surface area, A_o/a_f. The solid lines are derived from least-squares fits.

TABLE 2 Parameters obtained from plots of ln *f* versus A_o/a_f in DPPC bilayers (see Eq. 7)

Permeant	−slope	*r**
Formic acid	0.61 ± 0.05	0.97
Acetic acid	0.88 ± 0.06	0.98
Propionic acid	1.1 ± 0.2	0.94
Butyric acid	0.79 ± 0.30	0.85
Valeric acid	0.81 ± 0.10	0.97
Isovaleric acid	1.2 ± 0.3	0.95
Trimethylacetic acid	1.8 ± 0.2	1.00

*Correlation coefficient

tained for a similar plot of the slopes versus molecular volume (not shown).

The above results verify that Eq. 7 has the correct functional form. Thus the correction factor that accounts for the reduction in permeability in lipid bilayer membranes due to chain ordering is shown to depend exponentially on the ratio of permeant size to the free surface area of the membrane, both of which can be determined in independent experiments. We now consider the underlying molecular mechanisms that may account for the functional form of Eq. 7, with particular emphasis on the role of permeant size.

Previously, the effects of permeant size on permeability have been analyzed almost exclusively in terms of changes in permeant diffusivity (Stein, 1986; Walter and Gutknecht, 1986). In turn, our understanding of molecular diffusivity comes primarily from studies in simple liquids and polymers. Among many diffusion models, the free-volume concept has been most successful in describing various diffusion processes in simple liquids as well as in more complex polymers (Hildebrand, 1977; Vrentas, 1977). In the original diffusion theory of Cohen and Turnbull (Cohen and Turnbull, 1959; Turnbull and Cohen, 1970), translational diffusion of a molecule was assumed to occur when statistical redistribution of free volume opens up a cavity of a critical size in the immediate vicinity of the molecule. As a result, the diffusion coefficient D is proportional to the probability of finding a free volume with a size equal to or greater than that of the diffusant, V_s, which is usually assumed to be an exponential function:

$$D = D_o \exp(-\gamma V_s/V_f) \quad (9)$$

where D_o is a preexponential factor, γ is a constant to account for any overlap of free volumes, and V_f is the mean free volume. The Cohen-Turnbull theory has been used to predict the effects of permeant size on transport across both biological and model lipid bilayer membranes (Stein, 1986).

Galla (Galla et al., 1979) and later Vaz (Vaz et al., 1985a,b) and their co-workers modified the original free volume theory to describe the lateral diffusion of lipophilic probes in lipid bilayers in terms of free surface area rather than free volume. However, the dependence of permeant diffusive motion on molecular cross-sectional area rather than on molecular volume, as observed in studies of lateral diffusion in bilayers and in this study of transbilayer transport, is not unique to lipid bilayer membranes. Hildebrand and co-workers found that the diffusivity of dissolved gas molecules in bulk solvents depends on the cross-sectional area ($V^{2/3}$) of the diffusing molecules (Ross and Hildebrand, 1964). A study by Hayduk and Buckley (1972) also found that the bulk solvent diffusivities of linear or elongated molecules were in general higher than spherical or globular molecules with the same molar volume. Moreover, early studies of solute diffusion in polyisobutylene (Blyholder and Prager, 1960; Prager and Long, 1951) showed that the most elongated molecules have the highest diffusion rates (e.g., $D = 2.64$, 1.32, and 0.62×10^{-9} cm^2/s for *n*-pentane, isopentane, and neopentane, respectively), and straight-chain solutes have similar diffusion rates, regardless of their chain length (e.g., $D = 4.81$, 3.24, 2.64, 3.04, 3.16×10^{-9} cm^2/s for propane, *n*-butane, *n*-pentane, *n*-heptane, and *n*-octane, respectively). More recent studies by Vrentas (Vrentas and Vrentas, 1990) and others (Mauritz et al., 1990) further advanced the theory of Cohen and Turnbull by proposing that the elementary diffusive displacement may involve only a fraction of the total molecular length. As demonstrated in Fig. 8, because a solute molecule partitioned into the bilayer interior is preferentially oriented with its long axis along the bilayer normal (Mulders et al., 1986; Pope et al., 1984; Xiang and Anderson, 1994a), an effective transbilayer displacement may occur upon the opening of an adjacent free volume with a cross-sectional area equal to or greater than the minimum cross-sectional area of the diffusing permeant.

Whereas the effects of permeant size on permeability are typically treated in terms of changes in permeant diffusivity, large size effects on solute partitioning into interphases are evident by the high resolution attainable in chromatographic separations on the basis of subtle differences in the size and shape of the analyte (Wise et al., 1981). Schnitzer (1988) previously described the partitioning behavior of molecules into porous networks and membranes in terms of a free-

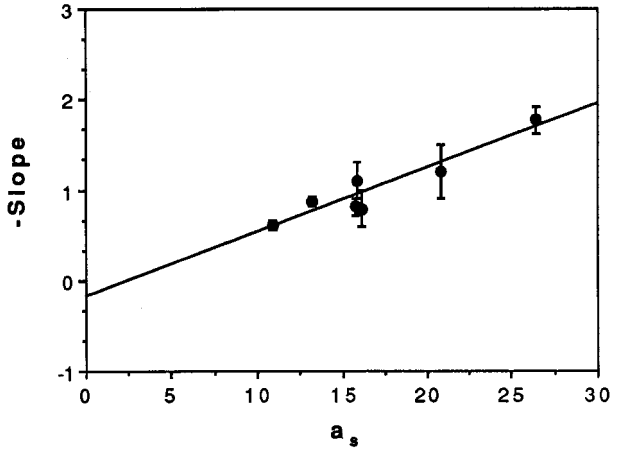

FIGURE 7 The correlation between the negative slopes for the ln f − A_o/a_f profiles obtained in Fig. 6 and the minimum cross-sectional areas for the monocarboxylic acid permeants.

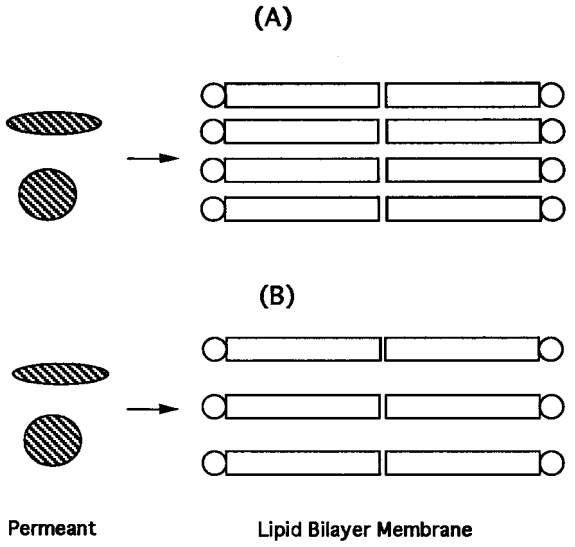

FIGURE 8 A schematic illustration of the effects of the free surface area of lipid bilayer membranes on the permeation of two permeants with the same molecular volume but different cross-sectional areas. (*A*) A lower free surface area. (*B*) A higher free surface area.

volume model in which the partition coefficient of a bilayer membrane can be expressed by an exponential function:

$$K_{\text{barrier/w}} = K_{\text{o}}\exp(-V_{\text{s}}/V_{\text{f}}) \qquad (10)$$

A statistical mechanical theory developed recently by the authors also suggests that solute partitioning into the barrier region of lipid bilayers is disfavored by chain ordering and that the selectivity of the barrier domain for permeant size is amplified with increases in surface density (i.e., decreases in free surface area) (Xiang and Anderson, 1994a). These results have been confirmed in molecular dynamics simulations, which have demonstrated a strong size dependence for solute partition coefficients in the order chain region in lipid bilayers (Marrink and Berendsen, 1996; Xiang and Anderson, 1998) and that the size dependence is amplified at high surface densities (data not shown). Experimentally, we have also shown that the size dependence of solute permeation across egg lecithin bilayers can be better described by a hybrid model incorporating the effects of solute size on both diffusion and partition coefficients, even though more adjustable parameters are involved (Xiang and Anderson, 1994b).

Whereas studies of size effects on partitioning have not explored the issue of whether the dependence of the partition coefficient in bilayers correlates better with solute volume or cross-sectional area, previous studies have shown that because of the ordering of lipid molecules in bilayer membranes, solute molecules residing in the bilayer interior are oriented with their long axes preferentially along the bilayer normal (Mulders et al., 1986; Pope et al., 1984; Xiang and Anderson, 1994a). Theoretically, this alignment minimizes the work required to create a cavity to accommodate the solute molecule in the lipid bilayer (Xiang and Anderson, 1994a). Thus the resistance to the transbilayer movement of a solute in the bilayer interior due to the partitioning term may depend primarily on the cross-sectional area along the long axis of the solute.

In summary, this study has systematically explored the effects of permeant size and bilayer chain packing on permeability across gel and liquid-crystalline DPPC bilayers, using a series of seven monocarboxylic acid permeants differing in chain length and degree of chain branching. First, we defined the permeability decrement f as the ratio of the observed permeability coefficients to those predicted by bulk solubility-diffusion theory to account for the decreases in permeability coefficients due to chain ordering. This chain-ordering correction factor was empirically shown to depend exponentially on the ratio of permeant cross-sectional area to the mean free surface area of the membrane. This strategy of investigating simultaneously the effects of permeant size on permeability in bilayers varying in packing density enables us to establish, for the first time, a model (cf. Eq. 7) that combines the effects of bilayer chain packing and permeant size on permeability across lipid bilayer membranes.

This work was supported by a grant from the National Institutes of Health (RO1 GM51347).

REFERENCES

Albery, W. J., A. R. Greenwood, and R. K. Kibble. 1967. Diffusion coefficients of carboxylic acids. *Trans. Faraday Soc.* 63:360–368.

Alger, J. R., and J. H. Prestegard. 1979. Nuclear magnetic resonance study of acetic acid permeation of large unilamellar vesicle membranes. *Biophys. J.* 28:1–14.

Anderson, B. D., and P. V. Raykar. 1989. Solute structure-permeability relationships in human stratum corneum. *J. Invest. Dermatol.* 93: 280–286.

Bangham, A. D., M. M. Standish, and J. C. Watkins. 1965. Diffusion of univalent ions across the lamellae of swollen phospholipids. *J. Mol. Biol.* 13:238–252.

Bar-On, Z., and H. Degani. 1985. Permeability of alkylamines across phosphatidylcholine vesicles as studied by ^{1}H-NMR. *Biochim. Biophys. Acta.* 813:207–212.

Bell, J. E. 1981. Spectroscopy in Biochemistry. CRC Press, Boca Raton, FL.

Blyholder, G., and S. Prager. 1960. The diffusion of hydrocarbons in polyisobutylene. *J. Phys. Chem.* 64:702–703.

Boden, N., S. A. Jones, and F. Sixl. 1991. On the use of deuterium nuclear magnetic resonance as a probe of chain packing in lipid bilayers. *Biochemistry.* 30:2146–2155.

Bondi, A. 1954. Free volumes and free rotation in simple liquids and liquid saturated hydrocarbons. *J. Phys. Chem.* 58:929–939.

Brahm, J. 1983. Permeability of human red cells to a homologous series of alphatic alcohols. *J. Gen. Physiol.* 81:283–304.

Bresseleers, G. J. M., H. L. Goderis, and P. P. Tobback. 1984. Measurement of the glucose permeation rate across phospholipid bilayers using smlal unilamellar vesicles. Effect of membrane composition and temperature. *Biochim. Biophys. Acta.* 772:374–382.

Brown, M. F., J. F. Ellena, C. Trindle, and G. D. Williams. 1986. Frequency dependence of spin-lattice relaxation times of lipid bilayers. *J. Chem. Phys.* 84:465–469.

Carruthers, A., and D. L. Melchior. 1983. Studies of the relationship between bilayer water permeability and bilayer physical state. *Biochemistry.* 22:5797–5807.

Chan, T. C. 1983. Diffusion of pseudospherical molecules: an investigation on the effects of dipole moment. *J. Phys. Chem.* 79:3591–3593.

Cohen, M. H., and D. Turnbull. 1959. Molecular transport in liquids and glasses. *J. Chem. Phys.* 31:1164–1168.

Davis, S. S., T. Higuchi, and J. H. Rytting. 1972. Determination of thermodynamics of the methylene group in solutions of drug molecules. *J. Pharm. Pharmacol.* 24(Suppl.):30P–46P.

Davis, S. S., T. Higuchi, and J. H. Rytting. 1974. Determination of thermodynamics of functional groups in solutions of drug molecules. *In* Advances in Pharmaceutical Sciences. Academic Press, London. 73–261.

de Gier, J., J. G. Mandersloot, J. V. Hupkes, R. N. McElhaney, and W. P. van Beek. 1971. On the mechanism of non-electrolyte permeation through lipid bilayers and through biomembranes. *Biochim. Biophys. Acta.* 233:610–618.

DeYoung, L. R., and K. A. Dill. 1988. Solute partitioning into lipid bilayer membranes. *Biochemistry.* 27:5281–5289.

DeYoung, L. R., and K. A. Dill. 1990. Partitioning of nonpolar solutes into bilayers and amorphous *n*-alkanes. *J. Phys. Chem.* 94:801–809.

Edward, J. T. 1970. Molecular volumes and the Stokes-Einstein equation. *J. Chem. Educ.* 47:261–270.

Fettiplace, R., and D. A. Haydon. 1980. Water permeability of lipid membranes. *Phys. Rev.* 60:510–550.

Finkelstein, A. 1976. Water and nonelectrolyte permeability of lipid bilayer membranes. *J. Gen. Physiol.* 68:127–135.

Galla, H.-J., W. Hartmann, U. Theilen, and E. Sackmann. 1979. On two-dimensional passive random walk in lipid bilayers and fluid pathways in biomembranes. *J. Membr. Biol.* 48:215–236.

Glasoe, P. K., and F. A. Long. 1960. Use of glass electrodes to measure acidities in deuterium oxide. *J. Phys. Chem.* 64:188–190.

Grant, D. J. W., and T. Higuchi. 1990. Solubility Behavior of Organic Compounds. John Wiley and Sons, New York.

Hanai, T., and D. A. Haydon. 1966. The permeability to water of bimolecular lipid membranes. *J. Theor. Biol.* 11:370–382.

Hayduk, W., and W. D. Buckley. 1972. Effect of molecular size and shape on diffusivity in dilute liquid solutions. *Chem. Eng. Sci.* 27:1997–2003.

Hayduk, W., and S. Ioakimidis. 1976. Liquid diffusivities in normal paraffin solutions. *J. Chem. Eng. Data.* 21:255–260.

Hildebrand, J. H. 1977. Viscosity and Diffusivity. John Wiley and Sons, New York.

Hine, J. 1975. Structural Effects on Equilibria in Organic Chemistry. John Wiley and Sons, New York. 168–172.

Jansen, M., and A. Blume. 1995. A comparative study of diffusive and osmotic water permeation across bilayers composed of phospholipids with different head groups and fatty acyl chains. *Biophys. J.* 68: 997–1008.

Klocke, R. A., K. K. Andersson, H. H. Rothman, and R. E. Forster. 1972. Permeability of human erythrocytes to ammonia and weak acids. *Am. J. Physiol.* 222:1005–1013.

Lande, M. B., J. M. Donovan, and M. L. Zeidel. 1995. The relationship between membrane fluidity and permeabilities to water, solutes, ammonia, and protons. *J. Gen. Physiol.* 106:67–84.

Lieb, W. R., and W. D. Stein. 1969. Biological membranes behave as non-porous polymeric sheets with respect to the diffusion of non-electrolytes. *Nature.* 224:240–243.

Lieb, W. R., and W. D. Stein. 1971. The molecular basis of simple diffusion within biological membranes. *Curr. Top. Membr. Transp.* 11:1–39.

Lieb, W. R., and W. D. Stein. 1986. Simple diffusion across the membrane bilayer. *In* Transport and Diffusion across Cell Membranes. Academic Press, Orlando, FL. 69–112.

Magin, R. L., and M. R. Niesman. 1984. Temperature dependent permeability of large unilamellar liposomes. *Chem. Phys. Lipids.* 34:245–256.

Marqusee, J. A., and K. A. Dill. 1986. Solute partitioning into chain molecule interphases: Monolayers, bilayer membranes, and micelles. *J. Chem. Phys.* 85:434–444.

Marrink, S. J., and H. J. C. Berendsen. 1994. Simulation of water transport through a lipid membrane. *J. Phys. Chem.* 98:4155–4168.

Marrink, S. J., and H. J. C. Berendsen. 1996. Permeation process of small molecules across lipid membranes studied by molecular dynamics simulations. *J. Phys. Chem.* 100:16729–16738.

Mauritz, K. A., R. F. Storey, and S. E. George. 1990. A general free volume based theory for the diffusion of large molecules in amorphous polymer above Tg. 1. Application to di-*n*-alkyl phthalates in PVC. *Macromolecules.* 23:441–450.

Meares, P. 1965. Polymers: Structure and Bulk Properties. Van Nostrand-Reinhold, Princeton, NJ.

Miller, K. W., L. Hammond, and E. G. Porter. 1977. The solubility of hydrocarbon gases in lipid bilayers. *Chem. Phys. Lipids.* 20:229–241.

Morrow, M. R., J. P. Whitehead, and D. Lu. 1992. Chain-length dependence of lipid bilayer properties near the liquid crystal to gel phase transition. *Biophys. J.* 63:18–27.

Mulders, F., H. van Langen, G. van Ginkel, and Y. K. Levine. 1986. The static and dynamic behaviour of fluorescent probe molecules in lipid bilayers. *Biochim. Biophys. Acta.* 859:209–218.

Nagle, J. F. 1993. Area/lipid of bilayers from NMR. *Biophys. J.* 64: 1476–1481.

Nemethy, G., I. Z. Steinberg, and H. A. Scheraga. 1963. Influence of water structure and hydrophobic interactions on the strength of side-chain hydrogen bonds in proteins. *Biopolymers.* 1:43–69.

Olson, F., C. A. Hunt, F. C. Szoka, W. J. Vail, and D. Papahadjopoulous. 1979. Preparation of liposomes of defined size distribution by extrusion through polycarbonate membranes. *Biochim. Biophys. Acta.* 557:9–23.

Overton, E. 1899. Ueber die allgemeinen osmotischen Eigenschaften der Zelle, ihre vermutlichen Ursachen und ihre Bedeutung fur die Physiologie. *Vjschr. Naturforsch. Ges. Zurich.* 44:88.

Papahadjopoulos, D., K. Jacobson, S. Nir, and T. Isac. 1973. Phase transitions in phospholipid vesicles. Fluorescence polarization and permeability measurements concerning the effect of temperature and cholesterol. *Biochim. Biophys. Acta.* 311:330–348.

Paula, S., A. G. Volkov, A. N. V. Hoek, T. H. Haines, and D. W. Deamer. 1996. Permeation of protons, potassium ions, and small polar molecules through phospholipid bilayers as a function of membrane thickness. *Biophys. J.* 70:339–348.

Perrin, D. D., and B. Dempsey. 1974. Buffers for pH and Metal Ion Control. Chapman and Hall, London.

Peters, R., and K. Beck. 1983. Translational diffusion in phospholipid monolayers measured by fluorescence microphotolysis. *Proc. Natl. Acad. Sci. USA.* 80:7183–7187.

Piette, L. H., and W. A. Anderson. 1959. Potential energy barrier determination for some alkyl nitrates by nuclear magnetic resonance. *J. Chem. Phys.* 30:899.

Pope, J. M., L. W. Walker, and D. Dubro. 1984. On the ordering of *n*-alkane and *n*-alcohol solutes in phospholipid bilayer model membrane systems. *Chem. Phys. Lipids.* 35:259–277.

Prager, S., and F. A. Long. 1951. Diffusion of hydrocarbons in polyisobutylene. *J. Am. Chem. Soc.* 73:4072–4075.

Rosen, H., A. Leaf, and W. B. Schwartz. 1964. Diffusion of weak acids across the toad bladder. Influence of pH on non-ionic permeability coefficients. *J. Gen. Physiol.* 48:379–389.

Ross, M., and J. H. Hildebrand. 1964. Diffusion of hydrogen, deuterium, nitrogen, argon, methane and carbon tetrafluoride in carbon tetrachloride. *J. Chem. Phys.* 40:2397–2399.

Sada, E., S. Katoh, M. Terashima, H. Kawahara, and M. Katoh. 1990. Effects of surface charges and cholesterol content on amino acid permeabilities of small unilamellar vesicles. *J. Pharm. Sci.* 79:232–235.

Sallee, V. L., and J. M. Dietschy. 1973. Determinants of intestinal mucosal uptake of short- and medium-chain fatty acids and alcohols. *J. Lipid Res.* 14:475–484.

Schnitzer, J. E. 1988. Analysis of steric partition behavior of molecules in membranes using statistical physics. Application to gel chromatography and electrophoresis. *Biophys. J.* 54:1065–1076.

Stein, W. D. 1986. Transport and Diffusion Across Cell Membranes. Academic Press, Orlando, FL.

Stein and Nir. 1971. On the mass dependence of diffusion within biological membranes and polymers. *J. Membr. Biol.* 5:246–249.

Tardieu, A., V. Luzatti, and F. C. Reman. 1973. Structure and polymorphism of the hydrocarbon chains of lipids: a study of lecithin-water phases. *J. Mol. Biol.* 75:711.

Todd, A. P., R. J. Mehlhorn, and R. I. Macey. 1989a. Amine and carboxylate spin probe permeability in red cells. *J. Membr. Biol.* 109:41–52.

Todd, A. P., R. J. Mehlhorn, and R. I. Macey. 1989b. Amine spin probe permeability in sonicated liposomes. *J. Membr. Biol.* 109:53–64.

Turnbull, D., and M. H. Cohen. 1970. On the free-volume model of the liquid-glass transition. *J. Chem. Phys.* 52:3038–3041.

Vaz, W. L. C., R. M. Clegg, and D. Hallmann. 1985a. Translational diffusion of lipids in liquid crystalline phase phosphatidylcholine multibilayers. A comparison of experiment with theory. *Biochemistry.* 24:781–786.

Vaz, W. L. C., D. Hallmann, R. M. Clegg, A. Gambacorta, and M. De Rosa. 1985b. A comparison of the translational diffusion of a normal and a membrane-spanning lipid in la phase 1-palmitoyl-2-oleoylphosphatidylcholine bilayers. *Eur. Biophys. J.* 12:19–24.

Venable, R. M., Y. Zhang, B. J. Hardy, and R. W. Pastor. 1993. Molecular dynamics simulations of a lipid bilayer and of hexadecane: an investigation of membrane fluidity. *Science.* 262:223–226.

Vrentas, J. S. 1977. Diffusion in polymer-solvent systems. I. Reexamination of the free-volume theory. *J. Polym. Sci.* 15:403–416.

Vrentas, J. S., and C. M. Vrentas. 1990. Influence of solvent size on the diffusion process for polymer-solvent systems. *J. Polym. Sci. Polym. Lett. Ed.* 28:379–383.

Walter, A., and J. Gutknecht. 1984. Monocarboxylic acid permeation through lipid bilayer membranes. *J. Membr. Biol.* 77:255–264.

Walter, A., and J. Gutknecht. 1986. Permeability of small nonelectrolytes through lipid bilayer membranes. *J. Membr. Biol.* 90:207–217.

White, S. H., G. I. King, and J. E. Cain. 1981. Location of hexane in lipid bilayers determined by neutron diffraction. *Nature.* 290:161–163.

Wise, S. A., W. J. Bonnett, F. R. Guenther, and W. E. May. 1981. A relationship between reversed-phase C_{18} liquid chromatographic retention and the shape of polycyclic aromatic hydrocarbons. *J. Chromatogr. Sci.* 19:457–464.

Worman, H. J., T. A. Brasitus, P. K. Dudeja, H. A. Fozzard, and M. Field. 1986. Relationship between lipid fluidity and water permeability of bovine tracheal epithelial cell apical membranes. *Biochemistry.* 25: 1549–1555.

Xiang, T.-X., and B. D. Anderson. 1994a. Molecular distributions in lipid bilayers and other interphases: a statistical mechanical theory combined with molecular dynamics simulation. *Biophys. J.* 66:561–573.

Xiang, T.-X., and B. D. Anderson. 1994b. The relationship between permeant size and permeability in lipid bilayer membranes. *J. Membr. Biol.* 140:111–121.

Xiang, T.-X., and B. D. Anderson. 1994c. Substituent contributions to the permeability of substituted *p*-toluic acids in lipid bilayer membranes. *J. Pharm. Sci.* 83:1511–1518.

Xiang, T.-X., and B. D. Anderson. 1995a. Development of a combined NMR paramagnetic ion-induced line-broadening/dynamic light scattering method for permeability measurements across lipid bilayer membranes. *J. Pharm. Sci.* 84:1308–1315.

Xiang, T.-X., and B. D. Anderson. 1995b. Phospholipid surface density determines the partitioning and permeability of acetic acid in DMPC: cholesterol bilayers. *J. Membr. Biol.* 148:157–167.

Xiang, T.-X., and B. D. Anderson. 1997. Permeability of acetic acid across gel and liquid-crystalline lipid bilayers conforms to free-surface-area theory. *Biophys. J.* 72:223–237.

Xiang, T.-X., and B. D. Anderson. 1998. Molecular dissolution processes in lipid bilayers: a molecular dynamics simulation. *J. Chem. Phys.* (in press).